# Conformation of Racemo and Meso Dyads in Glassy Polystyrenes from $^{13}C$ Polarization-Transfer NMR

**P. Robyr,*,† Z. Gan,‡ and U. W. Suter†**

*Department of Materials—Institute of Polymers and Department of Chemistry—Laboratory of Physical Chemistry, ETH, CH-8092 Zurich, Switzerland*

*Received July 7, 1998*

ABSTRACT: NMR measurements of polarization-transfer between carbon-13 nuclei in specifically labeled amorphous atactic and isotactic polystyrenes allow the conformational characterization of meso and racemo dyads separately. For racemo dyads, the experimental data are well explained by considering only conformations near those two used in rotational-isomeric-state (RIS) models. At least half of the racemo dyads in atactic polystyrene are near the *trans*−*trans* conformation. Calculations based on different RIS models for meso dyads are compared with measurements in isotactic polystyrene. RIS models with exclusively *trans*−*gauche* and *gauche*−*gauche* states fail to account for the measurements. RIS models with a small (5−10%), but significant, amount of meso dyads near the *trans*−*trans* state agree better with the experimental results. A comparison of the experimental data with calculations from atomistic simulations of atactic polystyrene shows that in the simulations, conformations which do not correspond to those considered in RIS models are overpopulated for both types of dyads.

## 1. Introduction

The basic understanding of chain conformation in glassy polymers borrows from studies of polymer conformations in solutions or in the melt and from energy calculations of short chain segments. Traditionally, the chain is thought to adopt a conformation close to that under Θ-conditions or in the melt.[1−3] In this view, the torsional angles of the backbone are close to a small number of values corresponding roughly to intramolecular energy minima. These considerations led to the formulation of the rotational-isomeric-state (RIS) theory.[2,3] However, a chain in glassy polymers is locked in a nonequilibrium state, and the interactions with other chain segments possibly affect its conformation, so that the description borrowed from isolated chains or melts may not apply. This opinion gained a foothold from the occurrence of chain conformations in dense atomistic simulations of several glassy polymers, which markedly differ from those of RIS models.[4−9] These differences were attributed to the dominance of intermolecular packing effects over those dictated by the local intramolecular interactions.

Recently, nuclear magnetic resonance (NMR) measurements in glassy bisphenol A polycarbonate[7] showed that the torsional angles of the carbonate groups obey the conformation distribution of the RIS model, and significantly deviate from the distributions found in atomistic simulations.[6,7] Differences between the chain conformation of RIS models[10,11] and that of atomistic simulations were also noticed in atactic polystyrene.[9] Validation of the atomistic models was attempted by comparing scattering intensities calculated from the model structures of polystyrene with intensities measured from neutron[9] and X-ray[12] scattering. However, scattering intensities are not specifically sensitive to the local chain conformations. Polarization-transfer rate constants measured with NMR in specifically labeled atactic polystyrene were compared with rate constants calculated from the atomistic models.[13] Significant differences were found between the two data sets, suggesting that the local order between the phenylene rings was not accounted for properly in the simulations. However, the specific origin of the disagreement could not be unraveled.

The purpose of this paper is to investigate to which extent the wide distribution of conformations found in atomistic simulations of atactic polystyrene occurs in the material. The investigation is based on polarization-transfer measurements between $^{13}C$ nuclei of specifically labeled atactic and isotactic glassy polystyrene samples (Figure 1). When measurements are performed in these two polymers, polarization transfer within the meso and the racemo dyads can be studied separately. To characterize the conformational disorder of the two dyads, the measurements are compared with calculations from atomistic simulations and RIS models. The comparison shows that the conformational disorder in the atomistic simulations is too large for both dyads. It also shows that chains with conformations close to those prescribed by intramolecular interactions well reproduce the experimental data of the racemo dyads but only partially account for the measurements in the meso dyads.

## 2. NMR Background

We consider an ensemble of nuclear spins-$^1/_2$ in a solid. The chemical shielding tensors of all spins have the same principal values but different orientations. The resonance frequencies vary from one spin to another only because of the different orientations of the spin-bearing molecular fragments. The dipolar couplings between the spins are much smaller than the range covered by the resonance frequencies. They give rise to an overall broadening in the observed spectra. This model applies to the system of $^{13}C$ labeled spins in polystyrene shown in Figure 1.

Polarization transfer from a group of spins A, with resonance frequencies between $\omega_A$ and $\omega_A + d\omega_A$, to a group of spins B, with resonance frequencies between

† Department of Materials—Institute of Polymers.
‡ Department of Chemistry—Laboratory of Physical Chemistry.

10.1021/ma981068q CCC: $15.00 
Published on Web 11/25/1998

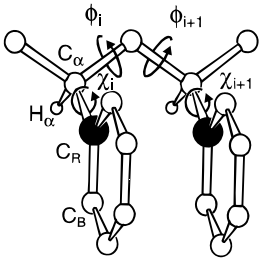


**Figure 1.** Meso dyad of polystyrene in the *trans-trans* conformations, $\phi_i = \phi_{i+1} = 0°$. Only the hydrogen bonded to $C_\alpha$ is shown. The torsional angle of the side group $\chi$:($H_\alpha$;$C_\alpha$;$C_R$;$C_B$) is zero in both monomer units. The black dots indicate the positions of the $^{13}$C-labeled carbons ($^{13}$C > 99%).

$\omega_B$ and $\omega_B + d\omega_B$, can be measured using two-dimensional NMR. If the polarization transfer between each pair of spins can be described by a rate constant, polarization transfer between the two groups of spins can also be quantified, in the initial rate regime, by a rate constant.[14] From rate constants measured under slow magic-angle-sample spinning (S-MAS),[15] the distance factors $f_d(\omega_A,\omega_B)$ can be extracted:[16,17]

$$f_d(\omega_A, \omega_B) = \frac{N}{n_A n_B} \sum_{i \in A} \sum_{j \in B} \frac{1}{r_{ij}^6} \qquad (1)$$

where $N$ is the total number of spins, $n_A$ and $n_B$ are the numbers of spins that belong to group A and group B, and $r_{ij}$ is the distance between spin $i$ and spin $j$. The double sum in eq 1 runs over the $n_A \times n_B$ pairs ($i$, $j$), with spin $i$ belonging to group A and spin $j$ to group B.

The distance factor can also be written as

$$f_d(\omega_A,\omega_B) = \frac{N}{n_B}\int_0^\infty N_{AB}(r) r^{-6}\, dr = \frac{N}{n_A}\int_0^\infty N_{BA}(r) r^{-6}\, dr \qquad (2)$$

where $N_{AB}(r)\, dr$ is the mean number of B spins at a distance between $r$ and $r + dr$ from an A spin, and $N_{BA}(r)\, dr$ is the mean number of A spins at a distance between $r$ and $r + dr$ from a B spin. An alternative formulation of the distance factor involves the pair correlation function $g_{AB}(r)$, where $4\pi g_{AB} r^2\, dr/V$ is the probability to find an A spin and a B spin at a distance between $r$ and $r + dr$; $V$ is the volume of the sample. The relation between the distance factor and the pair correlation function is

$$f_d(\omega_A,\omega_B) = 4\pi\rho\int_0^\infty g_{AB}(r) r^{-4}\, dr \qquad (3)$$

where $\rho = N/V$. In the absence of local orientational order between the spin-bearing molecular fragments, $g_{AB}(r)$ is equal for all pairs of resonance frequencies $\omega_A$ and $\omega_B$, and so is the distance factor $f_d$. Conversely, variations of the distance factor as a function of $\omega_A$ and $\omega_B$ reveal local order.

## 3. Experimental Section

Atactic polystyrene (a-PS) and isotactic amorphous polystyrene (i-PS) both selectively enriched with $^{13}$C (>99%) at position 1 in the phenylene ring (and $^{13}$C-depleted at the methylene carbon) were used in this study. A detailed description of the synthesis and the characterization of the polymers is given in ref 14. Labeled a-PS was prepared by free-radical polymerization of 1-$^{13}$C-$\beta$-$^{12}$C-styrene ($^{13}$C > 99%, $^{12}$C > 99.9%).[14] The polymer is characterized by $M_w = 105\,000$, $M_w/M_n = 1.7$ (size-exclusion chromatography with detectors for refractive index, light scattering and viscosity), and $T_g = 95$ °C. The NMR sample was prepared by annealing the polymer at 150 °C for 4 h. Labeled i-PS was prepared from polymerization of 1-$^{13}$C-$\beta$-$^{12}$C-styrene ($^{13}$C > 99%, $^{12}$C > 99.9%) with a supported Ziegler−Natta catalyst.[14] The polymer is characterized by $M_\eta = 1\,200\,000$ (viscosimetry, *o*-dichlorobenzene, 135 °C), tacticity ($m$) = 97% (NMR in solution), crystallinity = ca. 45% (X-ray), and $T_m = 220$ °C. Amorphous labeled i-PS was obtained by melting compact disks of ca. 20 mg of semicrystalline i-PS packed in aluminum containers in a bath of molten salts[18] at 250 °C for 3 min. Subsequently, the melt was quenched by dipping the containers in a bath of ice and water. No signs of crystallinity were detected in the quenched polymer, neither with X-ray nor with polarization transfer NMR.[14] The 1D $^{13}$C NMR spectra of the labeled polystyrenes are virtually equal. One of them is shown in Figure 2.

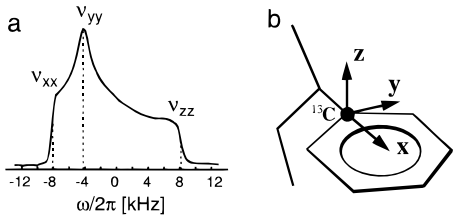


**Figure 2.** (a) $^{13}$C NMR spectrum at 298 K of glassy isotactic poly(1-$^{13}$C-$\beta$-$^{12}$C-styrene) ($^{13}$C > 99%, $^{12}$C >99.9%). The resonance frequencies corresponding to the principal values of the chemical-shielding-anisotropy tensor of the labeled carbon are indicated. (b) Orientation of the principal axes of the chemical-shielding-anisotropy tensor of the labeled carbon in poly(1-$^{13}$C-styrene) with respect to the molecular frame. The most shielded axis $z$ is perpendicular to the phenylene plane, and the least shielded axis $x$ is along the bond between the phenylene group and the main chain.

All NMR measurements were carried out at 298 K on a home-built spectrometer working at a proton frequency of 300 MHz using a Chemagnetics (Fort Collins, CO) 6 mm double resonance MAS probe. The rf fields on the $^{13}$C and the $^1$H channels were both matched at 62 kHz. The MAS frequency was 50 (±0.5) Hz. The 2D S-MAS polarization-transfer experiments follow the general scheme of 2D exchange spectroscopy.[15,19] The rf pulses and the sample rotation were synchronized so that the beginnings of evolution and detection occurred at the same rotor position. The evolution and detection periods were much shorter than the duration of a rotor cycle so that, along both axes of the 2D spectrum, the measured resonance frequencies correspond to those of a static sample.

The polarization-transfer rate constants used to calculate the distance factors[17] were obtained from a fit of a straight line to the off-diagonal intensities in the initial rate regime, scaled by the respective intensities of the quasi-equilibrium spectrum. For both polymers, six 2D polarization-transfer experiments were used with mixing times increasing from 20 to 120 ms in 20 ms steps. Scaled intensities larger than 0.4 were not considered. Longitudinal relaxation during the mixing time was negligible. The average intensities of the zero-quantum spectrum were evaluated from separated local field spectra as described in ref 15.

Additional 2D exchange experiments with proton decoupling during the mixing time were carried out without sample spinning. In these experiments, polarization transfer is quenched so that the presence of intensity in the off-diagonal region indicates reorientation processes of the labeled groups on the millisecond time scale. For both polystyrene samples, static experiments at 298 K with $\gamma_H B_{1H}/(2\pi) = 40$ kHz and a mixing time of 120 ms did not show any off-diagonal intensity. Therefore, motional contributions to the rate constants, cumulatively exceeding 5% of the measured values, could be ruled out.

The atomistic simulations used in this study were derived from 24 simulations of atactic polystyrene created by Rapold

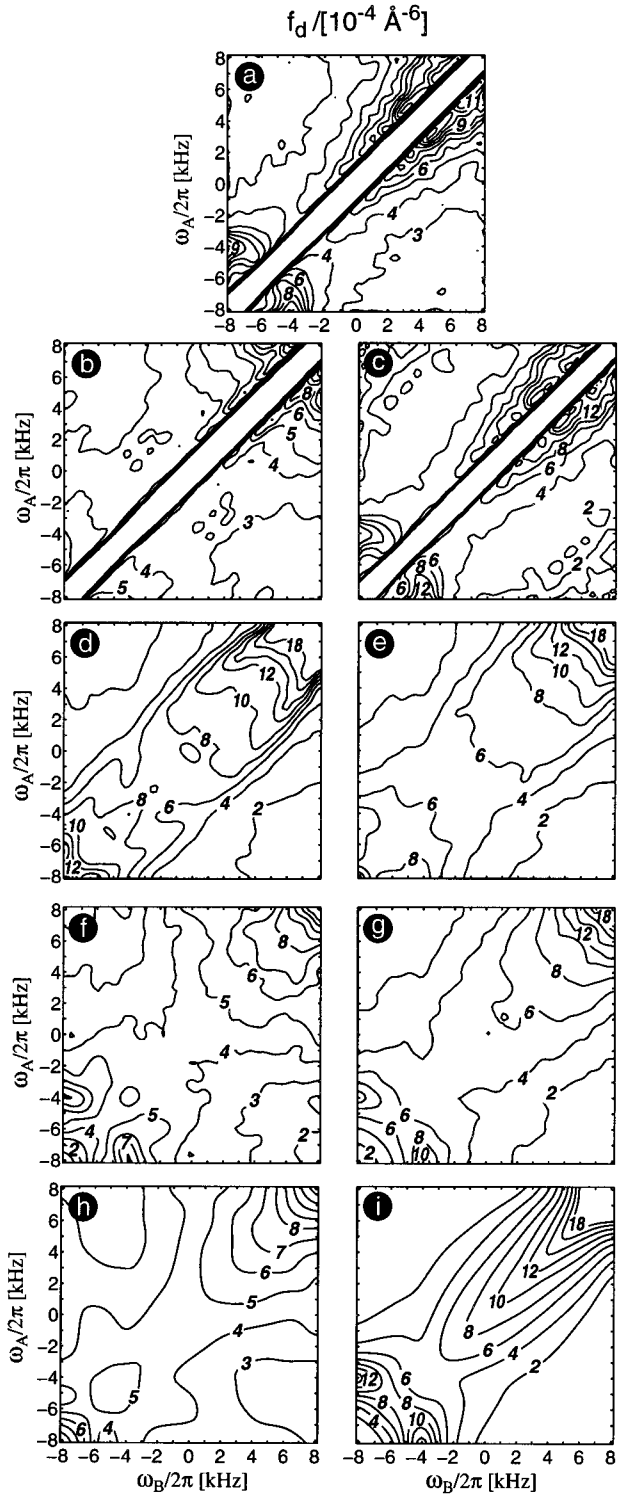


**Figure 3.** Distance factor $f_d$ as a function of the resonance frequencies $\omega_A$ and $\omega_B$ in glassy poly(1-$^{13}$C-styrene). Distance factors measured in atactic (a), $f_d^{aPS}$, and quenched isotactic (b), $f_d^{iPS}$, poly(1-$^{13}$C-$\beta$-$^{12}$C-styrene) at 298 K. (c) Distance factor of the racemo dyads in atactic poly(1-$^{13}$C-$\beta$-$^{12}$C-styrene), $f_d = (f_d^{aPS} - 0.48 f_d^{iPS})/0.52$. (d−i) Distance factors of meso and racemo dyads in poly-(1-$^{13}$C-styrene) calculated from atomistic simulations and from conformations of rotational-isomeric-state models. The orientation of the chemical-shielding-anisotropy tensor assumed in the calculations is shown in Figure 1, and the homogeneous line width of the experimental data was accounted for by convoluting the distance factors calculated in the delta-peak limit with a two-dimensional Gaussian function with a full width at half-height (fwhh) of 600 Hz. (d, e) Distance factors of the meso (d) and the racemo (e) dyads calculated from an average over 24 atomistic simulations of bulk a-PS. (f, g) Distance factors of the meso (f) and the racemo (g) dyads of the atomistic simulation that shows the best agreement with the corresponding experimental factors in parts b and c. (h) Distance factor of an ensemble of meso dyads with 80% of the dyads near the *tg* conformation, $\phi_i = 5°$ and $\phi_{i+1} = 115°$, 14% near the *gg* conformation, $\phi_i = \phi_{i+1} = 115°$, and 6% near the *tt* conformation, $\phi_i = \phi_{i+1} = 20°$. The distributions of the torsional angles of the side groups are centered at $\chi_i = \chi_{i+1} = 0°$. The distributions of all torsional angles are Gaussian with fwhh of 20° and uncorrelated. (i) Distance factor of an ensemble of racemo dyads where half of the dyads are near the *tt* conformation, $\phi_i = \phi_{i+1} = 5°$, and half near the *gg* conformation, $\phi_i = \phi_{i+1} = 115°$. The distributions of all torsional angles are Gaussian with fwhh of 20° and uncorrelated. The distributions of the torsional angles of the side groups are centered at $\chi_i = \chi_{i+1} = 0°$.

**Table 1. RIS Conformation Probabilities at 300 K of a Meso Dyad[a] in i-PS and a-PS**

| | Yoon et al.[10] | | Rapold and Suter[11] | |
|---|---|---|---|---|
| | i-PS | a-PS[b] | i-PS | a-PS[b] |
| *tt* | 0.13 | 0.07 | 0 | 0 |
| *tg* and *gt* | 0.87 | 0.92 | 1.00 | 0.99 |
| *gg* | 0.003 | 0.01 | <0.003[c] | 0.01 |

[a] The values are obtained from the conformation probabilities of the meso dyad in the middle of a chain of 100 monomers. [b] The values are averages over 100 chains with Bernoullian configuration distribution of the pseudo asymmetric centers, $p(l) = p(d) = 0.5$. [c] This value vanishes for infinitely long chain.

et al. and described in ref 9. Each of them is a periodically repeated box of edge length 18.65 Å that contains an atactic chain of 40 monomer units. Because carbon−carbon distances below 3 Å with correspondingly high van der Waals energies appeared in the structures of ref 9, the chain packings were "relaxed" using 25 ps molecular-dynamics (MD) runs flanked by two energy minimizations, each with 500 conjugated-gradients steps. In contrast to the force field with fixed bond angles and bond lengths used in ref 9, the unconstrained Cartesian-coordinate force field pcff91[20] was applied. The structure refinements were performed with the Discover program[21] at constant number of atoms, volume, and temperature (*NVT*) at 300 K. The time increment for the MD runs was 1 fs.

## 4. Results and Discussion

**4. I. Experimental Distance Factors.** The distance factors measured as a function of the resonance frequencies $\omega_A$ and $\omega_B$ in $^{13}C$ labeled a-PS and quenched i-PS are shown in parts a and b of Figure 3. Each labeled carbon has two neighbors at a distance between 3 and 5 Å, those of the dyads the considered carbon belongs to. The others labeled carbons are at distances larger than 5 Å. Since the contribution to the distance factor of each spin pair scales as the inverse sixth power of the internuclear distance (eq 1), we can consider the contributions from the ensemble of the dyads only. Further we assume that the contributions of the meso dyads in a-PS are the same as those in i-PS. This assumption is difficult to prove in general, but can be motivated by comparing the conformation probabilities of meso dyads in an isotactic and an atactic chain within the framework of RIS theory.[2,3] The a priori probabilities for *trans*−*trans* (*tt*), *trans*−*gauche* (*tg*) and *gauche*−*gauche* (*gg*) conformations of a meso dyad in i-PS and a-PS, calculated from the RIS models of Yoon, Sundararajan and Flory[10] and Rapold and Suter,[11] are listed in Table 1. The main difference is the lower *tt* probability in the atactic chain in the model of Yoon et al. However, these variations in the conformation probabilities are near the detection limit of the experimental results presented herein.

Assuming that only dyads contribute to the distance factors and that the contributions of meso dyads in i-PS and a-PS are equal, it is possible to separate the contributions from the racemo and the meso dyads to the distance factor measured in a-PS. Radically polymerized a-PS contains 52% of racemo and 48% of meso dyads;[22] therefore, the distance factor of the racemo dyads in a-PS is obtained from $f_d^{aPS} - 0.48 f_d^{iPS}$. This difference, divided by 0.52, so that the spin density is equal in all data sets, yields the distance factor in Figure 3c. The main differences between the distance factors of the racemo and the meso dyads are the peak at (−8, −4) kHz and the higher values of $f_d^{rac}$ close to the diagonal at high frequencies.

To interpret the distance factors in terms of local order, the orientation of the chemical shielding anisotropy (CSA) tensor of the labeled carbon is needed. For the labeled carbon of this study, the CSA orientation is well established.[23,24] The most shielded axis *z* is perpendicular to the phenylene plane, the least shielded axis *x* is along the bond that connects the side group to the main chain ($C_\alpha C_R$), and the intermediately shielded axis *y* is in the aromatic plane tangent to the ring (Figure 2b). The principal values of the CSA tensor are $\nu_{xx} = -8160$ Hz, $\nu_{yy} = 4280$ Hz, and $\nu_{zz} = 8160$ Hz, or $\delta_{xx} = 236$ ppm, $\delta_{yy} = 184$ ppm and $\delta_{zz} = 18$ ppm from TMS.

The high values of $f_d^{rac}$ (Figure 3c) close to the diagonal at high frequencies and the peak near ($\nu_{xx}$,$\nu_{yy}$) arise from racemo dyads in which the two phenylene rings are nearly coplanar and the two $C_\alpha C_R$ bonds are roughly at right angle. Such a situation occurs in a racemo dyad near the *tt* conformation. The high distance factor of i-PS (Figure 3b) in the region near ($\nu_{zz}$, $\nu_{zz}$) indicates that, in some meso dyads, small angles between two phenylene rings occur, but no sign of a localization of the angle between the two $C_\alpha C_R$ bonds can be found in the domain where the resonance frequencies are between $\nu_{xx}$ and $\nu_{yy}$. These qualitative interpretations can be made without requiring any detailed model. However, a quantitative analysis in connection with the conformation of the dyads must be based on a molecular model, since the distance factor is determined not only by the occurrence of a particular conformation but also by the distance between two labeled carbons of the dyad in that conformation.

**4. II. Comparison with Atomistic Simulations.** The distance factors of atomistically detailed simulations can be easily calculated according to eq 1. The distance factors of the meso and the racemo dyads calculated from an average over the 24 atomistic simulations described in the Experimental Section are shown in parts d and e of Figure 3. Both calculated distance factors differ significantly from the corresponding experimental data. The distance factor calculated from the meso dyads (Figure 3d) is too large near the diagonal and contains large peaks near ($\nu_{xx}$, $\nu_{xx}$) and ($\nu_{zz}$, $\nu_{zz}$). The distance factor calculated from the racemo dyads does not reproduce the peak near ($\nu_{xx}$, $\nu_{yy}$) observed experimentally.

The distance factors of each simulation were also compared to the experimental factors. For this purpose, the distance factors were averaged over six sets of coordinates sampled every 3 ps during a 15 ps MD run. The distance factors differ from one simulation to another. These variations are due to the limited number of dyads in a single simulation, and the impossibility of large rearrangements during the MD runs. The factors of the simulation that agree best with the experimental data are shown in parts f and g of Figure 3. The best agreement is found in the same structure for both dyads. This is probably a coincidence.

To rationalize the differences between the measured and the calculated distance factors, it is useful to consider the distribution of the torsional angles in the atomistic structures. The distributions of the two torsional angles $\phi_i$ and $\phi_{i+1}$ (Figure 1) in the meso and the racemo dyads of all 24 structures are shown in parts a and b of Figure 4. The two distributions obtained from the six sets of coordinates of the simulation whose distance factors agree best with the experimental ones

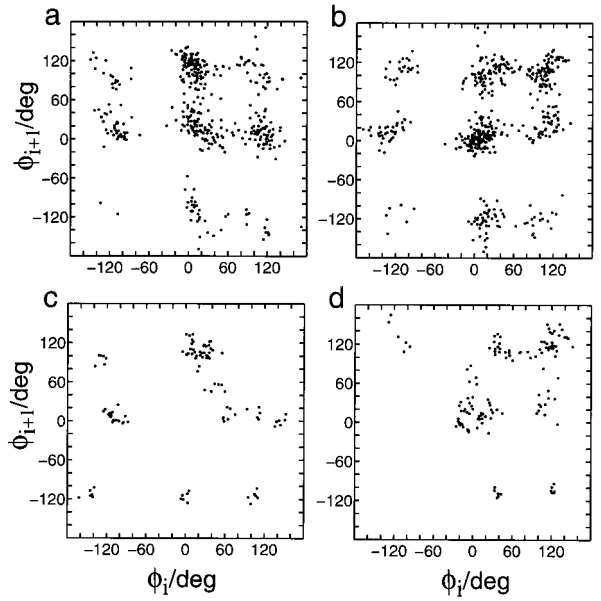


**Figure 4.** Torsional angles $\phi_i$ and $\phi_{i+1}$ of the meso and racemo dyads in the atomistic simulations of atactic polystyrene. (a, b) Torsional angles of the meso (a) and racemo (b) dyads of the 24 atomistic simulations. (c, d) Torsional angles of the meso (c) and the racemo (d) dyads of the atomistic simulation whose distance factors best agree with the measured distance factors (Figure 3). In parts c and d, the torsional angles obtained from six sets of coordinates sampled every 3 ps in a 15 ps MD run are shown.

are shown in parts c and d of Figure 4. The convention used to defined the sense of rotation of the torsional angles[10,11] is such that the same angles lead to the same molecular environments around the considered bond. Overall, the distributions in parts a and b of Figure 4 do not differ much despite the conspicuous differences in the energy surfaces calculated in meso and racemo 2,4-diphenylpentane as a function of the two torsional angles of the main chain.[11] The similarity of the distributions in parts a and b of Figure 4 indicates that, in the atomistic simulations of a-PS, the dyad conformations are strongly influenced by the packing of chain segments.

The high values of the distance factor calculated from the meso dyads of the 24 structures (Figure 3d) is due to the dyads (23%) near the *tt* conformation, $-60° \leq \phi_i$, $\phi_{i+1} \leq 60°$ (Figure 4a). Comparing models calculations with the experimental distance factor shows that the occurrence near the *tt* region should not exceed 10%. This condition is fulfilled by the "best" chain (Figure 4c). This chain contains about 50% of the meso dyads near the *gt*, (115, 5°), and *tg*, (5, 115°), conformations. It also contains about 25% of the meso dyads near the $\bar{g}t$, (115, 5°), and $t\bar{g}$, (5, −115°), conformations. These latter conformations are responsible for the weak peak of the distance factor near (−8, −4) kHz in Figure 3f. This peak does not appear in the distance factor measured in i-PS, so that the $\bar{g}t$ and $t\bar{g}$ regions are overpopulated in the atomistic simulations.

The weak peak near (−8, −4) kHz of the distance factor calculated from the racemo dyads of all 24 atomistic structures (Figure 3e) comes from the dyads near the *tt* conformation, $-30° \leq \phi_i, \phi_{i+1} \leq 30°$, in Figure 4b. These are 26% of all the racemo dyads. More dyads with conformations in that region are needed to account for the strong peak in the experimental data. A second peak, absent in the experimental distance factor, occurs near (−8, −6) kHz in Figure 3e. This peak arises from 17% of dyads whose conformations are in the $\bar{g}t$ and $t\bar{g}$ regions. Less than 8% of the dyads should adopt these conformations in order to reproduce the hole at (−8, −6) kHz in Figure 3c. The conformation distribution of the "best" chain (Figure 4d) fulfills both requirements mentioned above. However, even if this chain contains 36% of the dyads near the *tt* state, its distance factor at (−8, −4) kHz in Figure 3g is still smaller than the measured value.

**4. III. Comparison with RIS Models.** Several RIS models of a-PS exist.[25] In recent calculations,[11] the two lowest energy minima of the racemo dyads are located at (5, 5°) (*tt*) and (115, 115°) (*gg*), those of the meso dyads are found at (5, 115°) (*tg*) and equivalently (115, 5°) (*gt*) and at (105, 105°) (*gg*). Older RIS[10,25] models contain small amounts of meso dyads near the *tt* state (Table 1). Additional conformations are usually not considered in the models, because of their much higher energy. In all models, more than half of the racemo dyads are in the *tt* conformation and more than 85% of the meso dyads in the *tg* or *gt* conformations. No valid RIS model for strictly isotactic polystyrene is known.[10,11,25]

The distance factor calculated from a meso dyad in the *tg* conformation, assuming that the torsional angles of the side groups ($H_\alpha$;$C_\alpha$;$C_R$;$C_B$) are both 0°, reproduces well the distance factor measured in i-PS (Figure 3b) in the central region on both sides of the antidiagonal. However, it fails to account for the large values at low and high frequencies near the diagonal. The distance factor of a meso dyad in the *tg* conformation is very small in these regions ($f_d < 10^{-4}$ Å$^{-6}$), because in this conformation the angle between the two phenylene planes is large (≈60°). Variation of the conformation (± 20°) around the *tg* state and addition of a contribution from the *gg* conformation do not increase sufficiently the calculated distance factor near both extremities of the diagonal.

The location of the high values of the distance factor in Figure 3b indicates the presence of dyads with small angles between the two phenylene planes. To account for these arrangements, deviations of the orientations of the phenylene groups with respect to the main chain from those assumed above, or conformations in addition to *tg*, *gt*, and *gg* are necessary. Older RIS models[10,25] contain small amounts of meso dyads in the *tt* state (20, 20°). Adding the contributions of 6% of the dyads near the *tt* state, 80% near *tg*, and 14% near *gg* reproduces the experimental distance factor fairly well (Figure 3h). However, near both extremities of the diagonal, significant differences are still present.

While it is clear that *tg* and *gg* conformations are not sufficient to account for the distance factor measured in i-PS, the choice of the missing conformations is equivocal, especially because no precise information is available about the orientation of the side groups with respect to the backbone. The possibility shown in Figure 3h is one among others. For example, Keller et al.[26] postulated the occurrence of another conformation near the *tt* state where $(\phi_i, \phi_{i+1}) = (-23, 12°)$. Further experiments are necessary to clarify, which conformations near the *tt* state really occur.

The distance factor shown in Figure 3i is that of an ensemble of racemo dyads in which half of them are near the *tt* conformation and half near the *gg* conformation. The distribution of the torsional angles about the four bonds between two labeled carbons were assumed

to be uncorrelated and Gaussian with a fwhh of 20°. The contribution of the *tt* dyads to the distance factor dominates and generates all salient features in Figure 3i. This dominance comes from the much shorter distance between the two labeled carbons in the *tt* dyads than in the *gg* dyads, about 3.6 Å compared to about 5.0 Å. The factor calculated from the two conformations close to the RIS states reproduces the experimental data better than any of the 24 atomistic structures. Half of the dyads are required near the *tt* conformation to account quantitatively for the peak at (−8, −4) kHz. This quantity sets a lower bound for the content of racemo dyads near the *tt* conformation in a-PS, since the measurement of distance factors from polarization transfer in the initial rate regime tends to undervalue contributions from spin pairs with short internuclear distances.[16]

## 5. Conclusion

Measurements of polarization transfer between specifically labeled carbons in a-PS and i-PS indicate that the conformations of the meso and the racemo dyads in a-PS are close to those of RIS models, and show that some dyad conformations are strongly overpopulated in atomistic simulations[9] of a-PS. These erroneous conformation distributions likely result from exaggerated effects of the packing of chain segments in atomistic simulations.

Racemo dyads close to the *tt* and *gg* conformations of the RIS models suffice to reproduce the experimental distance factor. The experiments show that at least half of the racemo dyads are close to the *tt* state, and exclude substantial amounts (>8%) of $t\bar{g}$ and $\bar{g}t$ conformations. In the case of meso dyads, the experimental distance factor agrees with a large amount of dyads near the *tg* and *gt* conformations (>80%) and suggests the occurrence of a small amount (<10%) of dyads near the *tt* state.

The technique used in this study to characterize local conformational order is very sensitive to dyad conformations in which the distance between the two labeled carbons is short. This sensitivity results from the proportionality between the polarization-transfer rate constant and the inverse sixth power of the internuclear distance. Such a dependence has also its drawback. The sensitivity to dyads with long distances between the labeled carbons is low, and consequently, the conformational analysis is limited. Nevertheless, the results herein provide some clear details about the conformation in glassy polystyrenes and a sensitive check for atomistic simulations. They indicate the road to atomistic structures of glassy polystyrenes closer to reality.

**Acknowledgment.** This work was supported by the Swiss National Science Foundation. We thank Dr. Marcel Utz for valuable discussions, Dr. Marcel Zehnder and Dr. Roland Rapold for their help with the atomistic simulations, and Rolf Müller for the X-ray measurements. We also thank Prof. Richard R. Ernst for his support.

## References and Notes

(1) Flory, P. J. *Principles of Polymer Chemistry*, Cornell University Press: Ithaca, NY, 1953.
(2) Flory, P. J. *Statistical Mechanics of Chain Molecules*, reprinted ed.; Hanser Verlag: Munich, Germany, 1989.
(3) Mattice, W. L.; Suter, U. W. *Conformational Theory of Large Molecules*, Wiley: New York, 1994.
(4) Theodorou, D. N.; Suter, U. W. *Macromolecules* **1985**, *18*, 1467−1478.
(5) Ludovice, P. J.; Suter, U. W. In *Computational Modeling of Polymers*; Bicerano, J., Ed.; Marcel Dekker: New York, 1992; p 401.
(6) Hutnik, M.; Gentile, F. T.; Ludovice, P. J.; Suter, U. W.; Argon, A. S. *Macromolecules* **1991**, *24*, 5962−5969.
(7) Tomaselli, M.; Zehnder, M. M.; Robyr, P.; Grob-Pisano, C.; Ernst, R. R.; Suter, U. W. *Macromolecules* **1997**, *30*, 3579−3583.
(8) Khare, R.; Paulaitis, M. E.; Lustig, S. R. *Macromolecules* **1993**, *26*, 7203−7209.
(9) Rapold, R. F.; Suter, U. W.; Theodorou, D. N. *Macromol. Theory Simul.* **1994**, *3*, 19−43.
(10) Yoon, D.; Sundararajan, P. R.; Flory, P. J. *Macromolecules* **1975**, *6*, 776−783.
(11) Rapold, R. F.; Suter, U. W. *Macromol. Theory Simul.* **1994**, *3*, 1−17.
(12) Kotelyanskii, M.; Wagner, N. J.; Paulaitis, M. E. *Macromolecules* **1996**, *29*, 8497−8506.
(13) Robyr, P.; Tomaselli, M.; Grob-Pisano, C.; Meier, B. H.; Ernst, R. R.; Suter, U. W. *Macromolecules* **1995**, *28*, 5320−5324.
(14) Robyr, P.; Tomaselli, M.; Straka, J.; Grob-Pisano, C.; Suter, U. W.; Meier, B. H.; Ernst, R. R. *Mol. Phys.* **1995**, *84*, 995−1020.
(15) Gan, Z.; Ernst, R. R. *Chem. Phys. Lett.* **1996**, *253*, 13−19.
(16) Robyr, P.; Gan, Z. *J. Magn. Reson.* **1998**, *131*, 254−260.
(17) Robyr, P.; Gan, Z.; Suter, U. W. *Macromolecules* **1998**, *31*, 6199−6205.
(18) Hodgman, C. D., Ed., *Handbook of Chemistry and Physics*, The Chemical Rubber Publishing: Cleveland, OH, 1961; p 3424.
(19) Ernst, R. R.; Bodenhausen, G.; Wokaun, A. *Principles of Nuclear Magnetic Resonance in One and Two Dimensions*, Clarendon: Oxford, England, 1987.
(20) Maple, J. R.; Hwang, M.-J.; Stockfisch, T. P.; Dinur, U.; Waldman, M.; Ewig, C. S.; Hagler, A. T. *J. Comput. Chem.* **1994**, *15*, 162−182.
(21) Discover3.1 and InsightII, Biosym Technologies, Inc., San Diego, CA 1993.
(22) Williams, A. D.; Flory, P. J. *J. Am. Chem. Soc.* **1969**, *91*, 3111−3118.
(23) Mehring, M. *High-Resolution NMR in Solids*, Springer: Heidelberg, Germany, 1983.
(24) Veeman, W. S. *Prog. Nucl. Magn. Reson. Spectrosc.* **1984**, *16*, 193−235.
(25) Rehahn, M.; Mattice, W. L.; Suter, U. W. *Rotational Isomeric State Models in Macromolecular Systems*; Advances in Polymer Science 131/132, Springer: Berlin, 1997.
(26) Atkins, E. D. T.; Isaac, D. H.; Keller, A. *J. Polym. Sci. Polym. Phys. Ed.* **1980**, *18*, 71−82.

MA981068Q